CivilEng

MDPI

Article

Evaluation of Sequential Testing Strategies for Directional Compressive Strength of 3D-Printed Concrete Using Interlaboratory Data

Liuyang Ji [1,†], Shijie Soong [2,†], Zhe Hong [3], Zhilong Zhao [4,5] and Bo Nan [1,*]

[1] College of Water Conservancy, Shenyang Agricultural University, Shenyang 110866, China
[2] Department of Bioengineering, Royal School of Mines, Imperial College London, London SW7 2AZ, UK
[3] Principles of Informatics Research Division, National Institute of Informatics (NII), Tokyo 101-8430, Japan
[4] Biomanufacturing Center, Department of Mechanical Engineering, Tsinghua University, Beijing 100084, China
[5] Singapore Centre for 3D Printing, Nanyang Technological University, Singapore 639798, Singapore
* Correspondence: nanbo@syau.edu.cn
† These authors contributed equally to this work.

Abstract

The compressive strength of 3D-printed concrete (3DPC) varies with the loading direction, and the lowest-strength direction is not fixed across printing groups. Testing in a limited number of directions may miss the governing direction and bias the acceptance decision toward false acceptance. This study used the RILEM TC 304-ADC interlaboratory database comprising 27 laboratories, 34 printing groups, and 907 directional compressive test specimens. Exact sampling-without-replacement enumeration and leave-one-laboratory-out (LOLO) cross-validation were used to evaluate the relationships among directional coverage, false acceptance, and specimen consumption. The observed governing directions of the 34 printing groups were distributed across the U, V, and W directions. At an operational threshold of 40 MPa, the observed false-acceptance rates of the single-direction V3 and two-direction VW6 strategies were 13.7% and 10.6%, respectively, compared with 4.9% for the complete-direction UVW9 baseline. The early-acceptance strategy reduced the expected specimen count from 9.00 to 4.97, a reduction of 44.8%, but the observed false-acceptance rate increased from 4.93% to 9.15%. The risk difference was 4.22 percentage points, exceeding the 2.5-percentage-point screening criterion. Under the restricted-direction strategy, partial-direction results could trigger only early rejection, and final acceptance required complete U, V, and W directional evidence; the strategy therefore produced no acceptance decisions beyond those of the UVW9 baseline. In the present evaluation set, the restricted-direction strategy yielded group-by-group decisions identical to those of the UVW9 baseline, with an expected specimen count of 6.49, a reduction of 27.9% (95% interval 16.8% to 39.9%). Adaptive direction ordering saved 0.47 specimens relative to the original fixed order, and a simple fixed order that tests the most frequently governing direction first achieved the same saving; the overall savings arose primarily from printing groups that did not meet the strength requirement. Overall, the results show that cross-directional historical information can optimize the testing order and identify nonconforming printing groups earlier, whereas final acceptance should continue to require complete directional evidence. In production settings where staged specimen preparation and testing are feasible, this procedure could reduce the cost of destructive testing and bring forward the review and process correction of anomalous printing groups.

Keywords: 3D-printed concrete; quality control; directional compressive strength; sequential testing; false acceptance; interlaboratory evaluation

Check for updates

Academic Editors: Angelo Luongo and Akanshu Sharma

Received: 23 August 2026
Revised: 7 September 2026
Accepted: 9 September 2026
Published: 11 September 2026

Copyright: © 2026 by the authors. Licensee MDPI, Basel, Switzerland. This article is an open access article distributed under the terms and conditions of the Creative Commons Attribution (CC BY) license.

1. Introduction

3D-printed concrete (3DPC) is fabricated by a layer-by-layer extrusion-deposition process that creates interfaces between successively deposited layers and between adjacent filaments within the same layer, producing a hardened material with a distinct bedding structure and filament orientation [1,2]. When test specimens are extracted from a printed element along different directions, each loading direction bears a distinct geometric relationship to the layer-plane normal and the printing path. The loading direction parallel to the printing path is conventionally designated U, the transverse in-plane loading direction is designated V, and the loading direction normal to the deposited layers is designated W [3,4]. This internal structure causes the compressive strength of 3DPC to vary with the loading direction. For conventionally cast concrete, by contrast, standard macroscopic compressive tests do not typically treat the loading direction as an independent sampling dimension [5,6].

Previous studies have shown that the compressive strength, elastic modulus, and failure mode of 3DPC can all vary with the loading direction [4,7,8]. Interlayer bonding quality, pore distribution between deposited layers, and the orientation of printed filaments or reinforcing fibers are the principal factors contributing to directional differences [9–11]. Specimens loaded normal to the deposited layers are generally more susceptible to interlayer-interface-governed failure, but studies have not reached consistent conclusions on which loading direction exhibits the lowest compressive strength [4,10,12]. Variations in mix design, printing parameters, specimen size, sampling location, and curing conditions can all alter the magnitude of the directional effect and the ranking of directional strengths [4,12,13]. Consequently, a direction that exhibits a lower mean strength at the population level does not necessarily govern the acceptance decision for every individual print run.

The interlaboratory mechanical-property study organized by RILEM TC 304-ADC compiled directional compressive strength data from laboratories operating with their own material systems and printing equipment [3,4]. That study revealed substantial differences among laboratories in overall strength level, magnitude of directional variation, and testing variability, as well as differences in material composition, extrusion equipment, printing parameters, and specimen preparation methods. The interlaboratory data thus provide broader condition coverage than single-laboratory experiments, while also indicating that directional strength rankings obtained from a specific material or a single laboratory should not be directly generalized to other printing conditions.

Existing research on directional mechanical behavior has focused primarily on the strength levels in different loading directions and on the mechanisms underlying directional differences. Quality testing, by contrast, must address a different question: whether test results from a limited number of directions are sufficient to determine that the lowest directional strength of a printing group meets a specified requirement. In this study, the set of specimens produced from a single print run and serving as one quality-decision unit is referred to as a printing group. For a given printing group, the minimum of the arithmetic mean strengths in the U, V, and W directions defines the governing strength, and the corresponding direction is termed the observed governing direction. The observed governing direction is determined by the available test data and is not equivalent to a fixed intrinsic weak direction of the material system. If testing covers only a subset of directions, the observed governing direction of a given printing group may be missed. The strength estimated from the tested directions can then exceed the complete-direction governing strength, biasing the acceptance decision toward false acceptance.

This problem can be framed as the following testing scenario. A printing group whose strength conformance is in question requires directional compressive testing to determine whether its lowest directional strength meets a specified threshold. With three specimens

per direction, as adopted in this study, complete testing in the U, V, and W directions requires nine specimens. Directional compressive testing is destructive; each additional direction increases both specimen preparation and testing effort. If historical data can identify directions that are more likely to reveal a low-strength condition, the testing order may be adjusted to reach a decision earlier for some printing groups. However, a high strength in the tested directions does not by itself rule out the possibility that an untested direction falls below the threshold. Reducing specimen consumption must therefore be evaluated jointly with directional coverage and the risk of incorrect decisions.

In this testing scenario, the consequences of the two types of misclassification are asymmetric. Falsely accepting a printing group that does not meet the strength requirement may compromise the effectiveness of quality control and affect subsequent structural reliability. Falsely rejecting a conforming printing group primarily increases the costs of retesting, specimen preparation, and material consumption. Conventional concrete strength acceptance procedures typically weigh both false-acceptance and false-rejection risks, controlling decision performance through within-batch sample size, mean strength, standard deviation, and operating characteristic curves [14–16]. Bayesian methods can further incorporate historical data to update strength distribution parameters and express decision uncertainty under limited specimen availability [17,18]. These methods provide a foundation for risk-based strength acceptance but generally treat specimens within the same batch as exchangeable replicate observations drawn from a single population.

Sequential acceptance methods add specimens incrementally and use the accumulated evidence to decide whether to continue or stop testing, thereby balancing decision risk against testing effort [19–21]. Directional testing of 3DPC differs from traditional sequential sampling in one important respect: each additional test provides an observation in a new loading direction rather than a replicate within the same direction. Statistical associations may exist among the U, V, and W directions, yet each direction remains a distinct, non-interchangeable candidate for the governing direction of a printing group. Cross-directional associations revealed by historical data can help determine the testing order but may not substitute for direct observation of an untested direction. In directional testing, therefore, the choice of the first tested direction and the stopping rule require separate evaluation.

Against this background, existing research has not adequately addressed the following three interrelated questions. First, whether population-level directional rankings can provide a reliable basis for direction selection in individual printing groups, and to what extent reducing directional coverage increases the risk of missing the observed governing direction and of false acceptance. Second, whether cross-directional statistical associations can support early acceptance when partial-direction results are favorable, while maintaining acceptable decision performance under held-out laboratory conditions. Third, whether historical data used only to optimize the testing order and to enable early rejection of nonconforming printing groups, with early acceptance disallowed, can reduce specimen consumption while introducing no acceptance decisions beyond the complete-direction baseline. These questions jointly concern the quantitative relationship among directional coverage, decision risk, and specimen consumption. Relative to existing sequential acceptance sampling and Bayesian conformity methods, which treat additional specimens as exchangeable observations from a single population, this study contributes a sequential acceptance framework that treats each printing direction as a distinct candidate for the governing strength. A leave-one-laboratory-out evaluation then quantifies its false-acceptance risk and specimen consumption on interlaboratory data.

This study used directional compressive strength data from the RILEM TC 304-ADC interlaboratory database to evaluate sequential testing strategies for 3DPC. The analysis proceeded at two levels. First, exact sampling-without-replacement enumeration was

performed on all 34 printing groups to compare single-direction, two-direction, and complete three-direction strategies in terms of observed governing direction omission, strength overestimation, and false-acceptance rate. This comparison quantified the effect of reduced directional coverage on the acceptance decision. Second, LOLO cross-validation was used to compare the early-acceptance strategy, the restricted-direction strategy, and the complete-direction baseline UVW9 in terms of false-acceptance rate and specimen consumption, while distinguishing the contributions of testing order and stopping rule. These analyses addressed the limits of cross-directional statistical associations in acceptance decisions: whether such associations can prioritize the testing direction and support early rejection of some nonconforming printing groups, and whether they can replace direct observation of untested directions when confirming acceptance.

2. Data Source and Evaluation Baseline

This study used directional compressive strength data from the RILEM TC 304-ADC interlaboratory mechanical-property study [3,4,22]. The data were organized at four hierarchical levels: laboratory, printing group, loading direction, and specimen. The printing group, the set of specimens produced from a single print run, is the acceptance decision unit. The laboratory serves as the partitioning unit for LOLO cross-validation and as the clustering unit for interval estimation. Individual specimens constitute replicate observations within a specific printing group and loading direction. The inclusion criteria were as follows: default process parameters as labeled in the database; a testing age of 26 to 30 d; valid compressive strength results reported in MPa; and no fewer than three valid specimens in each of the U, V, and W directions for the same printing group. Printing groups that did not satisfy the three-direction completeness requirement were excluded, and no outlier removal was performed. Under these criteria, the final dataset comprised 34 printing groups from 27 laboratories, totaling 907 directional specimens. Cast companion specimens were excluded from the directional analysis because they carry no printing direction and cannot inform the U/V/W acceptance decision. Where printed and cast specimens were both available, the mean strength of the cast specimens generally exceeded the governing directional strength of the corresponding printing group, so considering them separately does not alter the interpretation of the directional results. Seven laboratories each contributed two printing groups, and the remaining 20 laboratories each contributed one. The specimen counts by direction are given in Table 1.

The complete-direction reference decision was based on all available specimens in the U, V, and W directions for each printing group. The arithmetic mean of the specimen strengths was first computed separately for each direction, and the minimum of the three directional means was taken as the governing strength, with the corresponding direction defined as the observed governing direction. For a fixed single direction, the difference between that directional mean and the governing strength of the same printing group is termed the strength overestimation. It measures how far a single-direction assessment can overstate the governing strength. Under a given strength threshold, a printing group was classified as reference-conforming if its governing strength was not lower than the threshold, and as reference-nonconforming otherwise. Conformity is defined here relative to the evaluation threshold only and does not indicate compliance with a design code or project requirement. This reference classification served as the uniform benchmark for evaluating the decisions of different testing strategies. Under the operational thresholds determined in each cross-validation round, 18 of the 34 printing groups were reference-nonconforming and 16 were reference-conforming. Of the cross-validation rounds, 24 used 40.0 MPa (28 held-out printing groups) and 3 used 37.5 MPa (6 held-out printing groups). The training-data selection rule for the operational threshold is described in Section 3.5. These thresholds served to construct evaluation conditions with approximately balanced reference categories, and should

be interpreted as statistical evaluation points produced by this balancing rule rather than as design values; the acceptance threshold in a specific engineering application should be determined according to project requirements.

Table 1. Interlaboratory dataset and evaluation units.

Item	Value	Notes
Laboratories (inferential clustering unit)	27	Clustering unit for every interval estimate reported in this study.
Complete U/V/W printing groups (evaluation unit)	34	One held-out evaluation unit per printing group; 7 laboratories contribute 2 groups, 20 contribute 1.
U/V/W specimens	907 (U 301, V 299, W 307)	163 CAST specimens excluded from the directional analysis; primary cohort total 1070.
Reference-nonconforming printing groups (at per-round operational thresholds)	18	Denominator of the false-acceptance rate.
Reference-conforming printing groups	16	Denominator of the false-rejection events.
Per-round primary operational threshold	Per-round rule; observed: 40.0 MPa (28 groups), 37.5 MPa (6 groups)	Prespecified per round as the training pass rate closest to 0.50, ties resolved to the lower threshold: 40.0 MPa in 24 rounds (28 printing groups), 37.5 MPa in 3 rounds (6 printing groups). There is no single universal threshold.
Direction block	3 specimens per direction	Block size fixed in advance; sequential policies act in whole blocks.
Complete-direction baseline (UVW9)	9 specimens	3 directions × 3 specimens; the comparator of the single primary comparison.
Outer validation	Leave-one-laboratory-out, 27 rounds	Threshold selection, hyperparameters and direction selection all exclude the held-out laboratory.
Observed governing-direction counts U/V/W	4/20/10	Print-group level; at the laboratory level, the counts are 4/15/8. The governing direction is not invariant across laboratories.

Specimens are repeated measurements within printing group and direction, not independent inferential units; all interval estimates cluster by laboratory (27 clusters).

3. Methods

Three categories of strategies were designed for comparative evaluation. Fixed-direction strategies prespecified a direction combination for one-time testing. The early-acceptance strategy could make either an acceptance or a rejection decision after testing only a subset of directions, based on the posterior conformance probability. The restricted-direction strategy prohibited early acceptance based on partial-direction results; final acceptance still required complete directional evidence. All sequential strategies were evaluated under LOLO cross-validation (Figure 1).

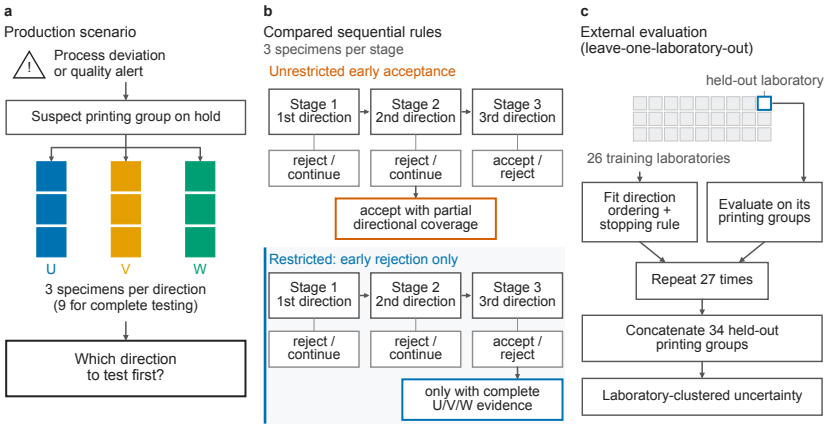


Figure 1. Study framework for directional compressive-strength acceptance testing of 3DPC: (**a**) production scenario and U/V/W specimen blocks; (**b**) unrestricted and restricted sequential decision rules; and (**c**) LOLO cross-validation across 27 laboratories. Each testing stage comprises three specimens; final acceptance under the restricted strategy requires complete U/V/W evidence.

3.1. Fixed-Direction Strategies

Fixed-direction strategies were used to characterize the effect of directional coverage on the false-acceptance rate. The analysis examined all three single-direction strategies (U3, V3, W3), all three two-direction strategies (UV6, UW6, VW6), and the complete three-direction strategy UVW9, for a total of seven combinations. The decision rule for each strategy compared the minimum of the specimen means across the selected directions with the threshold. V3 had the lowest false-acceptance rate among single-direction strategies in the present dataset; among two-direction strategies, no alternative combination achieved both a lower false-acceptance rate and a lower specimen count than VW6. Both selections were determined by the current data and cannot be directly generalized to other material systems or printing conditions. The fixed-direction results were obtained by exact sampling-without-replacement enumeration across all 34 printing groups, without probabilistic models or LOLO cross-validation; they were therefore evaluated at a different level from the sequential strategies described below.

3.2. Probabilistic Model and Posterior Updating

The sequential strategies employed a trivariate normal working model for the latent log-mean strengths [23]. This approximate model computes posterior conformance probabilities and guides direction selection; it is not intended as a complete description of the data-generating process. For the three latent log-mean strengths $\boldsymbol{\mu} = (\mu_U, \mu_V, \mu_W)^\top$ of a printing group from a new laboratory, the working prior was

$$\boldsymbol{\mu} \sim N_3(\boldsymbol{m}_0, \boldsymbol{\Sigma}_0), \tag{1}$$

where $\boldsymbol{m}_0 = (\alpha, \alpha + \beta_V, \alpha + \beta_W)^\top$ and $\boldsymbol{\Sigma}_0 = \boldsymbol{\Sigma}_B + \sigma_L^2 \mathbf{1}\mathbf{1}^\top$. Here, α is the median estimate of the population-level intercept for the U direction, β_V and β_W are the median estimates of the log-mean differences relative to the U direction, σ_L is the between-laboratory standard deviation (estimated as 1.4826 × MAD, where MAD denotes the median absolute deviation), and $\boldsymbol{\Sigma}_B$ is the sample covariance of the laboratory-location-centered printing-group direction vectors (with $10^{-6}\boldsymbol{I}$ added to ensure positive definiteness). Parameters were estimated in each cross-validation round using only the training laboratories. Arithmetic means of the raw specimen strengths were computed first and then log-transformed. With 34 printing groups, 20 of which come from laboratories contributing a single group, $\boldsymbol{\Sigma}_B$ (and in particular its correlation structure) is estimated with limited precision; the influence of

the estimation method on the strategy evaluation is examined in Section 3.7. The adequacy of this working approximation was examined with marginal and multivariate normality diagnostics of the group-level log-mean strengths (Figure S1).

The testing unit for each direction was a directional specimen set of three specimens. Let $z_d = \log(\bar{X}_d)$ denote the log of the arithmetic mean of the three specimens in direction d. With the set of observed directions denoted O, the working likelihood was $\boldsymbol{z}_O = \boldsymbol{H}_O\boldsymbol{\mu} + \boldsymbol{\varepsilon}_O$, where $\boldsymbol{\varepsilon}_O \sim N(\boldsymbol{0}, \sigma_e^2/k \cdot \boldsymbol{I})$, $k = 3$, and $\boldsymbol{H}_O$ is the direction selection matrix. The within-group residual standard deviation σ_e was computed from the differences between individual specimen log-strengths and the log mean for the corresponding printing group and loading direction, estimated as 1.4826 × MAD; when the MAD fell below a numerical floor of 10^{-4} (in log units), the sample standard deviation was used instead [24].

The posterior distribution was

$$\boldsymbol{\Sigma}_O = (\boldsymbol{\Sigma}_0^{-1} + \boldsymbol{H}_O^{\top}\boldsymbol{R}^{-1}\boldsymbol{H}_O)^{-1}, \tag{2}$$

$$\boldsymbol{m}_O = \boldsymbol{\Sigma}_O(\boldsymbol{\Sigma}_0^{-1}\boldsymbol{m}_0 + \boldsymbol{H}_O^{\top}\boldsymbol{R}^{-1}\boldsymbol{z}_O), \tag{3}$$

where $\boldsymbol{R} = \sigma_e^2/k \cdot \boldsymbol{I}$. The posterior conformance probability was defined as

$$p_O(T) = \Phi_3(\boldsymbol{m}_O - \log(T)\boldsymbol{1}; \boldsymbol{0}, \boldsymbol{\Sigma}_O), \tag{4}$$

where $\Phi_3(\boldsymbol{a}; \boldsymbol{0}, \boldsymbol{\Sigma})$ is the joint probability that a zero-mean trivariate normal variable is componentwise no greater than $\boldsymbol{a}$. Even when only a subset of directions had been observed, this probability was computed over all three directions, with unobserved directions extrapolated through the prior covariance structure. The multivariate normal joint probability was computed using the SciPy numerical algorithm [25,26], with a fixed random seed to ensure reproducibility across runs. In practical terms, $p_O(T)$ is the model-based probability that every directional mean strength of the printing group meets the threshold, given the directions tested so far.

3.3. Sequential Testing Strategies and Stopping Rules

Both sequential strategies used directional specimen sets of three specimens as the testing unit and proceeded through at most three testing stages. After each direction was tested, the trivariate joint posterior distribution was updated using the observed directions, and the posterior conformance probability was used to decide whether to stop testing or to add the next direction. The two strategies shared the same direction selection method and the same early-rejection threshold but differed in whether early acceptance was permitted based on partial-direction results, and in the final decision rule after all three directions had been tested.

The early-acceptance strategy operated under the following rules: at Stage 1, if $p_1 \leq 0.10$, the group was rejected; otherwise, the second direction was tested. At Stage 2, if $p_2 \geq 0.90$, the group was accepted; if $p_2 \leq 0.10$, the group was rejected; otherwise, the third direction was tested. At Stage 3, if $p_3 \geq 0.65$, the group was accepted; otherwise, the group was rejected. Acceptance was thus possible only from Stage 2 onward. The Stage 3 criterion differs from the UVW9 rule, which compares the minimum of the three directional specimen-set means with the threshold (Table 2). Table S1 reports the operating characteristics under neighboring combinations of the acceptance and rejection confidence levels.

Table 2. Testing strategy definitions.

Strategy	Direction Selection	Early Rejection	Early Acceptance	Complete U/V/W Evidence Required for Acceptance	Maximum Specimens	Role in Study
V3 [1]	Single fixed direction V	No	No	No	3	Baseline [4]
VW6 [1]	Two fixed directions V, W	No	No	No	6	Baseline [4]
UVW9 [1]	All three directions	No	No	Yes	9	Reference comparator [5]
Fixed-order early-acceptance strategy	Prespecified order W–V–U	Yes (from Stage 1)	Yes (from Stage 2) [2]	No	9	Secondary comparison [6]
Adaptive early-acceptance strategy	Adaptive order [3]	Yes (from Stage 1)	Yes (from Stage 2) [2]	No	9	Primary comparison [7]
Fixed-order restricted-direction strategy	Prespecified order W–V–U	Yes (from Stage 1)	Not permitted	Yes	9	Secondary comparison [6]
Adaptive restricted-direction strategy	Adaptive order [3]	Yes (from Stage 1)	Not permitted	Yes	9	Secondary comparison [6]

[1] V3, VW6, and UVW9 are single-stage strategies: all specimens are tested at once, so staged early rejection and early acceptance do not arise. UVW9 tests all three directions by design. [2] Early acceptance from Stage 2 onward may be reached with partial-direction coverage. [3] Adaptive order: The first direction is selected using training-laboratory data and the second is selected using path-specific one-step lookahead. [4] Incomplete-coverage baselines, included to illustrate the acceptance risk of testing fewer than three directions. [5] Complete-direction engineering baseline; comparator of the single prespecified primary comparison. [6] Secondary comparisons: The fixed-order variants keep the prespecified W–V–U direction order, and the adaptive restricted-direction strategy was prespecified as a secondary comparison with early acceptance not permitted. The fixed-order early-acceptance strategy did not meet the false-acceptance point-estimate criterion (Table 3). [7] The only prespecified primary comparison; the false-acceptance point-estimate criterion was not met (Table 3). Notes: Sequential strategies act in blocks of 3 specimens per direction; Stage 1 cannot accept (the earliest acceptance stage is Stage 2); acceptance/rejection thresholds were specified before analysis. Final-stage rules differ: Early-acceptance strategies decide at Stage 3 using posterior probability ($\geq$0.65); restricted-direction strategies and UVW9 accept only if every direction-block mean meets the threshold.

Table 3. False-acceptance rates and specimen consumption for the main strategies.

Strategy	Observed FA (%) [1]	FA 95% Interval (%) [2]	FA Diff. vs. UVW9 (pp) [4]	FA Diff. 95% Interval (pp)	Expected Specimens	Expected Specimens 95% Interval	Specimen Reduction vs. UVW9 (%)	False-Rejection Events [1]	Prespecified Assessment/Role [6]
Complete-direction baseline (UVW9)	4.9	[0.4, 10.8]	—	—	9	fixed by design	0	0 of 16	Complete-direction comparator
Fixed-order early-acceptance strategy	9.1	[0.2, 23.2]	4.2	[−2.9, +18.3]	5.44	[4.91, 5.90]	39.6 [34.4, 45.4]	0 of 16	Secondary fixed-order comparison; false-acceptance point-estimate criterion not met
Adaptive early-acceptance strategy [7]	9.1	[0.2, 23.2]	4.2	[−2.9, +18.3]	4.97	[4.43, 5.45]	44.8 [39.5, 50.8]	0 of 16	Only prespecified primary comparison; false-acceptance point-estimate criterion not met; conclusion sensitive to omitting Laboratory 18124

Table 3. *Cont.*

Strategy	Observed FA (%) [1]	FA 95% Interval (%) [2]	FA Diff. vs. UVW9 (pp) [4]	FA Diff. 95% Interval (pp)	Expected Specimens	Expected Specimens 95% Interval	Specimen Reduction vs. UVW9 (%)	False-Rejection Events [1]	Prespecified Assessment/Role [6]
Fixed-order restricted-direction strategy	4.9	[0.4, 10.8]	0	identical decisions [3]	6.96	[5.99, 7.81]	22.7 [13.2, 33.4]	0 of 16	Secondary comparison; 25% specimen-reduction point-estimate criterion not met
Fixed V–W–U restricted-direction strategy	4.9	[0.4, 10.8]	0	identical decisions [3]	6.47	[5.39, 7.48]	28.1 [16.9, 40.1]	0 of 16	Secondary fixed-order comparison; 25% specimen-reduction point-estimate criterion met
Adaptive restricted-direction strategy	4.9	[0.4, 10.8]	0	identical decisions [3]	6.49 [5]	[5.41, 7.49]	27.9 [16.8, 39.9]	0 of 16	Prespecified secondary comparison; early acceptance not permitted; 25% specimen-reduction point estimate met

[1] FA = false acceptance among the 18 reference-nonconforming printing groups; FR events counted among the 16 reference-conforming printing groups; per-round primary operational thresholds (40.0 MPa for 28 printing groups, 37.5 MPa for 6). [2] Intervals: Laboratory-clustered bootstrap 95% percentile intervals (10,000 replications, 27 clusters, shared resample indices across strategies and a random seed fixed in advance). No p-values by design. [3] The restricted-direction strategies (all three orderings) cannot add acceptances relative to UVW9 on matched sampling paths because early acceptance is not permitted and final acceptance uses the UVW9 rule. In this cohort they also produced identical decisions to UVW9; this sample equality does not establish zero population difference and the strategies may add false rejections in other data. [4] The 2.5-percentage-point value is a prespecified point-estimate screening criterion, not a formal non-inferiority margin. For the adaptive early-acceptance strategy, the observed increment was 4.2 points, so the criterion was not met. Its paired 95% interval $[-2.9, +18.3]$ crosses both 0 and 2.5 points; the population direction and magnitude therefore remain uncertain. [5] For the adaptive restricted-direction strategy, the expected-specimen point estimate was 6.49 and met the 25% reduction criterion (≤ 6.75). Its 95% interval $[5.41, 7.49]$ includes values above 6.75, so the efficiency conclusion remains uncertain. Expressed as a reduction, the point estimate of 27.9% has a 95% interval of 16.8% to 39.9%, which spans the 25% benchmark; the reduction should therefore be read as a point-estimate result for the present evaluation set rather than an established performance level. [6] Criterion 3 was assessed in the prespecified implementation as FA not exceeding UVW9 (proxy for "no unacceptable weakest-direction deterioration"). [7] The adaptive early-acceptance strategy was the only prespecified primary comparison. Fixed-order and restricted-direction strategies are secondary comparisons. Omitting Laboratory 18124 reverses the primary conjunction, indicating single-laboratory sensitivity; this does not alter the full-cohort point estimates reported above.

The restricted-direction strategy retained the early-rejection rule when the posterior conformance probability did not exceed 0.10 at Stage 1 or Stage 2, but did not allow early acceptance based on partial-direction results. Printing groups that did not trigger early rejection in the first two stages were required to complete all three directions, with the final decision made according to the same rule as UVW9.

The decision property of the restricted-direction strategy can be expressed as follows. For any given sampling realization ω, the UVW9 acceptance decision is

$$D_{\mathrm{UVW9}}(\omega) = \mathbf{1}\left[\min_{d} \bar{X}_{d,3}(\omega) \geq T\right]. \tag{5}$$

Defining the event that early rejection was not triggered in the first two stages as $S(\omega) = \mathbf{1}[R_1(\omega) = 0, R_2(\omega) = 0]$, the final acceptance decision of the restricted-direction strategy is

$$D_{\mathrm{lim}}(\omega) = S(\omega) D_{\mathrm{UVW9}}(\omega). \tag{6}$$

Because $S(\omega) \in \{0, 1\}$, for any given sampling realization, $D_{\mathrm{lim}}(\omega) \leq D_{\mathrm{UVW9}}(\omega)$, and consequently $\mathrm{FA}_{\mathrm{lim}} \leq \mathrm{FA}_{\mathrm{UVW9}}$. The restricted-direction strategy therefore accepts only printing groups that UVW9 would also accept. Conversely, early rejection may increase the false-rejection risk for reference-conforming printing groups, i.e., $\mathrm{FR}_{\mathrm{lim}} \geq \mathrm{FR}_{\mathrm{UVW9}}$.

3.4. Direction Testing Order

The direction testing order was determined from the training-laboratory data, with the first direction selected to minimize the expected classification loss [27]. The loss function for an immediate decision was defined as

$$L(p) = \min\{c_{\mathrm{FA}}(1 - p), c_{\mathrm{FR}} p\}, \tag{7}$$

where c_{FA} and c_{FR} denote the relative costs of a false acceptance and a false rejection. The weights were set for consistency with the final decision rule: at Stage 3, a printing group is accepted when its posterior conformance probability is at least 0.65, and choosing $c_{\mathrm{FA}} = 0.65$ and $c_{\mathrm{FR}} = 0.35$ places the indifference point of $L(p)$, $p^* = c_{\mathrm{FA}}/(c_{\mathrm{FA}} + c_{\mathrm{FR}}) = 0.65$, at this same probability, so that direction selection and the final decision express the same trade-off between the two error types. Table S1 examines the joint influence of the weights and this cutoff.

The first direction was determined separately for each cross-validation round and each candidate threshold. For each printing group in the training laboratories, the expected loss corresponding to the empirical specimen-set mean distribution of each candidate direction was computed. When the number of three-specimen subsets did not exceed 200, exact enumeration was used; when it exceeded 200, a reproducible random sample of 200 subsets was drawn with a fixed seed. The expected loss was averaged first within printing groups and then equally across training printing groups. The direction with the lowest average loss was selected as the first direction; in case of a tie, the directions were ranked in the following order: U, V, W. The second direction was determined by a one-step-ahead expected loss minimization based on the posterior predictive distribution along each testing path, using the nine-node Gauss–Hermite quadrature. This one-step-ahead computation used a scalar grid of 257 equally spaced nodes extending 2% of the observed range beyond both endpoints, with piecewise cubic Hermite interpolation (PCHIP) [28]; the resulting probabilities were clipped to $[0, 1]$. The random seed was determined by fixed indices of the held-out laboratory, candidate threshold, direction, and printing group.

Of the 296 first-direction selections determined by the training data, the V direction accounted for 96%; the remainder were W.

3.5. Leave-One-Laboratory-Out Evaluation and Operational Threshold

The sequential strategies were evaluated using LOLO cross-validation [29,30], comprising 27 rounds. In each round, one laboratory and all its printing groups served as the evaluation data, while the remaining 26 laboratories were used for model parameter estimation, direction selection, and operational threshold determination. Each printing group was evaluated through 10,000 finite-population sampling-without-replacement paths, with each path drawing three specimens within a direction. Table S1 reports the stability of the results from 1000 to 20,000 paths and under two alternative random seeds. All strategies used the same printing groups, operational thresholds, and sampling paths, enabling paired comparison. Across the 27 rounds, each printing group entered the evaluation exactly once.

The operational threshold in each round was determined solely from the training laboratories. The candidate threshold range was 20 to 100 MPa in increments of 2.5 MPa. A threshold entered the candidate set when the training data contained at least eight reference-conforming and at least eight reference-nonconforming printing groups. From the candidate set, the threshold producing a training reference-conforming rate closest to 0.50 was selected; in case of a tie, the lower value was chosen. This rule was designed to produce an evaluation operating point with approximately balanced reference categories. In engineering applications, the strength threshold is an external design condition that should be determined according to specific project requirements before testing.

3.6. Evaluation Metrics and Decision Criteria

The observed false-acceptance rate was defined as the conditional proportion of reference-nonconforming printing groups classified as conforming by the testing strategy, with a denominator of 18 reference-nonconforming printing groups. The observed false-rejection rate was defined as the conditional proportion of reference-conforming printing groups incorrectly classified as nonconforming, with a denominator of 16 reference-conforming printing groups. The expected specimen count was the average specimen consumption per printing group over 10,000 sampling paths. Interval estimation used laboratory-clustered percentile bootstrap [31,32] with 10,000 resamples. The resampling units were the held-out evaluation results formed in each round; model parameters, direction ordering, and operational thresholds were held fixed during resampling. Strategy comparisons were paired as described in Section 3.5, and both point estimates and 95% intervals are reported.

The overall assessment of the early-acceptance strategy comprised five conditions: (1) expected specimen count no greater than 6.75; (2) observed false-acceptance rate no greater than 5%, or the increment relative to UVW9 no greater than 2.5 percentage points; (3) observed false-acceptance rate no greater than that of UVW9; (4) the direction of the risk difference between the early-acceptance strategy and UVW9 remained consistent under different reference-decision definitions; and (5) upon sequentially removing the held-out evaluation records of each laboratory, the joint assessment of Conditions (1) through (3) remained unchanged. All five conditions had to be satisfied simultaneously. The 2.5-percentage-point value was adopted as a prespecified screening criterion applied to the point estimate, set before the analysis at one half of the 5% false-acceptance design target, and was not a formal non-inferiority margin. The 95% interval was used to characterize estimation uncertainty. Condition (3) imposed a stricter constraint on the same false-acceptance metric and used the same risk-evaluation data as Condition (2). Condition (4) examined four reference-decision definitions: complete-sample mean, median, 10% trimmed mean, and hierarchical latent mean.

3.7. Robustness and Applicability Analyses

To assess the sensitivity of the conclusions to the held-out results of individual laboratories, the held-out evaluation records contributed by each laboratory were removed in turn, and the expected specimen count, observed false-acceptance rate, and joint assessment of Conditions (1) through (3) were recomputed. This analysis was based on existing cross-validation predictions without re-estimating the model parameters, direction ordering, or operational thresholds for the remaining rounds.

To examine the influence of the parameter estimation method on strategy evaluation, hyperparameters were estimated using Markov chain Monte Carlo (MCMC) in each cross-validation round, replacing the robust empirical estimates [33,34]. This analysis employed a Student-t hierarchical model for specimen log-strengths, incorporating laboratory effects, printing-group effects, and within-group direction contrasts. The population intercept prior was $N(3.5, 0.5^2)$; the population-level V and W differences relative to U used $N(0, 0.20^2)$ priors. The log-priors for the laboratory, printing-group, and residual standard deviations were all normal with a standard deviation of 0.7, with means of -1.85, -2.05, and -2.05, respectively. The direction-contrast covariance used an LKJ correlation prior ($\eta = 1$) [35] and log-normal marginal standard deviation priors (log-mean -2.75, log-standard deviation 0.7). The Student-t degrees-of-freedom log-prior was $N(\log 8, 1)$. Each round ran four chains with 1500 warmup iterations and 1000 retained iterations per chain, a target acceptance rate of 0.99, and a maximum tree depth of 12; the posterior medians were substituted into the decision model. This analysis used the same stopping rules and operational threshold selection method as the original evaluation. Parameter-level convergence diagnostics (R-hat and bulk and tail effective sample sizes) were computed for every round. Because several rounds exceeded common limits under these settings (maximum R-hat above 1.01 or minimum effective sample sizes below 400), the analysis was repeated for all rounds with reinforced sampling (4000 retained draws and 4000 warmup iterations per chain); Table S2 reports the diagnostics of both runs, and Section 4.4 describes the influence on the results.

To examine the influence of the reference-conforming rate of the testing population on specimen consumption, the conditional expected specimen counts for reference-conforming and reference-nonconforming groups were computed separately. Letting the reference-conforming rate of the testing population be q, the overall expected specimen count was

$$E\{N(q)\} = qE(N \mid \text{pass}) + (1 - q)E(N \mid \text{fail}). \tag{8}$$

A 25% reduction in specimen count relative to the nine-specimen complete-direction testing corresponds to $E\{N(q)\} \leq 6.75$, and the corresponding reference-conforming-rate boundary is

$$q_{25} = \frac{6.75 - E(N \mid \text{fail})}{E(N \mid \text{pass}) - E(N \mid \text{fail})}. \tag{9}$$

Additionally, to distinguish the contributions of the direction ordering and the stopping rule to specimen consumption, the expected specimen counts of the restricted-direction strategy were compared under three orderings: the prespecified W–V–U order, a fixed V–W–U order in which the direction most often governing in this dataset is tested first, and adaptive ordering. Paired differences among the orderings were computed from per-group evaluation results on identical sampling paths, and the influence of the reference-conforming rate on the overall expected specimen count was analyzed to identify the conditions under which the restricted-direction strategy remains specimen-efficient.

4. Results

4.1. Distribution of Observed Governing Directions and Single-Direction Strength Overestimation

Among the 34 printing groups, the observed governing direction was V in 20 groups (58.8%), W in 10 groups (29.4%), and U in 4 groups (11.8%). No single direction consistently corresponded to the observed governing direction across the 34 printing groups. Fitted to the complete dataset, the hierarchical model of Section 3.7 gave population-level directional strength ratios of 0.879 for V relative to U (95% interval 0.861 to 0.897), 0.941 for W relative to U (0.923 to 0.959), and 1.071 for W relative to V (1.050 to 1.092); the average anisotropy is therefore moderate compared with the group-to-group variation that determines the governing direction. Figure 2a shows the directional overestimation for each printing group, defined as the difference between each directional mean and the governing strength of the respective group; at least one direction in each group had an overestimation of zero. The maximum single-direction overestimation was approximately 28 MPa. When only a single direction was tested, the observed governing direction was missed in 88.2%, 41.2%, and 70.6% of groups for U, V, and W, respectively, with corresponding mean strength overestimations of 8.14, 3.00, and 5.72 MPa (Figure 2b).

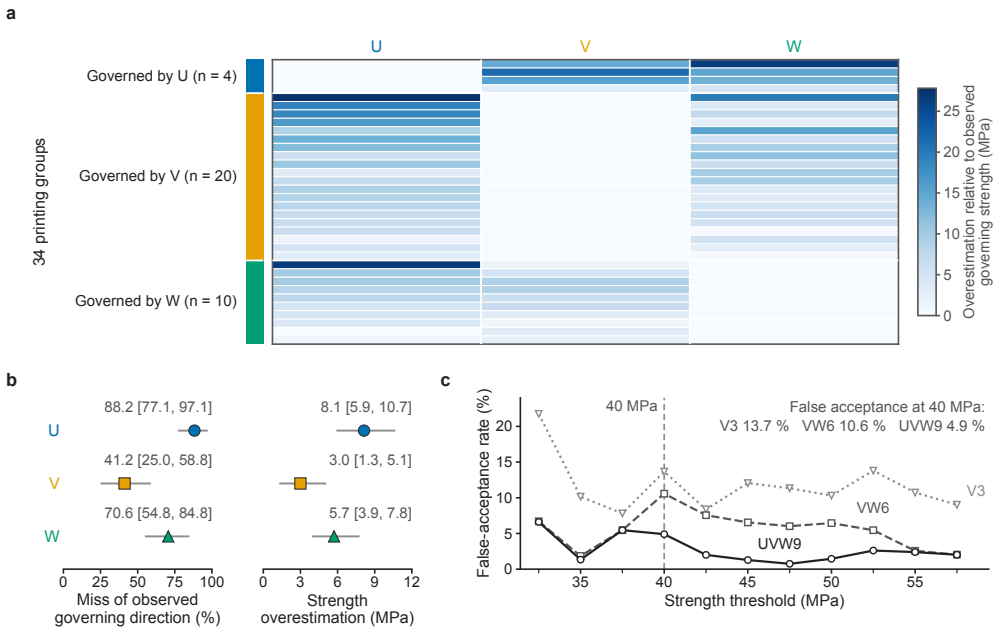


Figure 2. Directional variability and consequences of incomplete testing across 34 printing groups: (**a**) directional overestimation relative to each group's governing strength, with rows grouped by observed governing direction (colour strip at the left: blue for U, orange for V, green for W) and cell shading read from the colour bar; (**b**) missed-governing-direction proportions and overestimation magnitudes with laboratory-clustered 95% intervals, in which circles denote the U direction, squares the V direction and triangles the W direction, and each annotation gives the point estimate followed by its 95% interval in square brackets; and (**c**) false-acceptance rates for V3, VW6, and UVW9 across the effective threshold range, in which V3 is drawn as a light grey dotted line with open downward triangles, VW6 as a grey dashed line with open squares, and UVW9 as a black solid line with open circles. The vertical dashed line marks the 40 MPa operational threshold.

4.2. False-Acceptance Rates Under Different Directional Coverage Strategies

Exact enumeration showed that the fixed-direction strategies differed in false-acceptance rate across the effective threshold range of 32.5 to 57.5 MPa (Figure 2c). At 40.0 MPa, the false-acceptance rates for V3, VW6, and UVW9 were 13.7%, 10.6%, and 4.9%, respectively. At 37.5 MPa, VW6 and UVW9 had equal false-acceptance rates; at all

other effective thresholds, the false-acceptance rate of VW6 exceeded that of UVW9. The number of reference-nonconforming printing groups, and hence the denominator of the false-acceptance rate, varied with the threshold.

4.3. Decision Performance of the Early-Acceptance Strategy

The adaptive sequential strategy permitting early acceptance lowered the expected specimen count from 9.00 to 4.97, a 44.8% reduction (Table 3, Figure 3a). The observed false-acceptance rate of this strategy was 9.15%, compared with 4.93% for UVW9, yielding a difference of 4.22 percentage points between the two overall decision strategies. This difference exceeded the screening criterion of 2.5 percentage points, and the observed rate of 9.15% exceeded the 5% risk target; the strategy therefore did not meet the prespecified criteria. The paired 95% interval for the risk difference was $[-2.90, 18.30]$ percentage points, crossing both zero and the 2.5-percentage-point screening criterion. No false-rejection events were observed among the 16 reference-conforming printing groups.

Of the five assessment conditions, Condition (1) was satisfied: the expected specimen count was below 6.75. The false-acceptance rate and its increment relative to UVW9 did not meet the requirements of Conditions (2) and (3). All four reference-decision definitions (complete-sample mean, median, 10% trimmed mean, and hierarchical latent mean) produced 18 reference-nonconforming and 16 reference-conforming printing groups, satisfying Condition (4). Upon removal of the held-out evaluation records of Laboratory 18124, the joint assessment of Conditions (1) through (3) changed, and thus Condition (5) was not satisfied. The strategy therefore did not satisfy the five assessment conditions jointly. This assessment was unchanged under every sensitivity setting examined in Table S1.

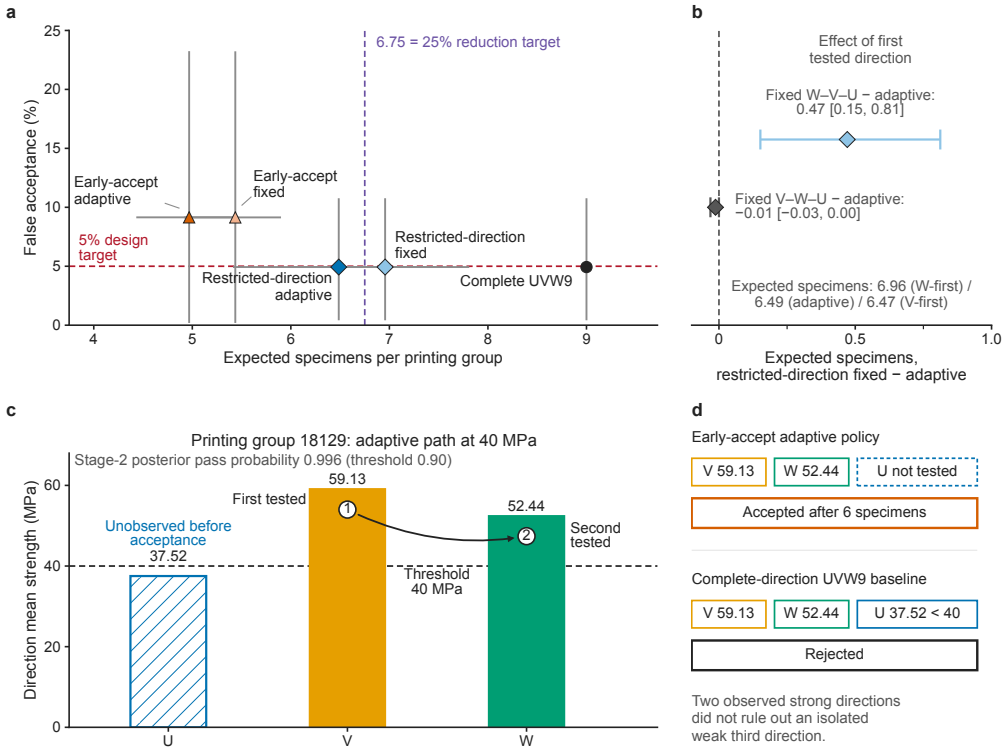


Figure 3. Performance of sequential testing strategies: (**a**) observed false-acceptance rate and expected specimen count with laboratory-clustered 95% intervals, shown as grey whiskers; triangles denote the early-acceptance strategies (filled for adaptive ordering, pale for fixed order), diamonds the restricted-direction strategies (dark for adaptive ordering, light for fixed order) and the filled circle the complete-direction UVW9 baseline; the red horizontal dashed line marks the 5% false-acceptance

design target and the purple vertical dashed line the 6.75-specimen level that corresponds to a 25% reduction; (**b**) paired differences in expected specimens of the restricted-direction strategy for the prespecified W–V–U (light blue diamond) and the fixed V–W–U (grey diamond) orders relative to adaptive ordering, with horizontal whiskers giving laboratory-clustered 95% intervals and the vertical dashed line at zero indicating no difference; (**c**) testing path for printing group 18129 at 40 MPa, in which the hatched bar is the U direction that was still unobserved when acceptance was reached, the circled numbers give the testing order and the horizontal dashed line marks the 40 MPa threshold; and (**d**) the corresponding false-acceptance pathway under early acceptance, in which a dotted outline marks an untested direction, an orange frame an acceptance decision and a black frame a rejection decision.

4.4. Parameter Estimation Sensitivity

When the hyperparameters in each round were replaced by MCMC posterior median estimates from the Student-t hierarchical model, the observed false-acceptance rate of the early-acceptance strategy was approximately 9.34%, that of UVW9 remained at 4.93%, and the expected specimen count was approximately 5.00. The assessment status of the five conditions was the same as under the robust empirical estimates. Parameter-level diagnostics identified 12 of the 27 rounds with at least one metric outside its limit: the maximum R-hat exceeded 1.01 in 9 rounds, the minimum bulk effective sample size fell below 400 in 5, and the minimum tail effective sample size fell below 400 in 11, with no divergent transitions in any round (Table S2) [36,37]. After reinforced sampling, every round met all three limits; the false-acceptance rate moved by less than 0.01 percentage points, the expected specimen count was unchanged to two decimal places, and the first tested direction was unchanged in every round.

4.5. An Illustrative False-Acceptance Path and Laboratory Influence

Printing group 18129 was from Laboratory 18124, with an operational threshold of 40 MPa. The U-direction mean strength of this group was 37.52 MPa, below the threshold; the V- and W-direction means were 59.13 and 52.44 MPa, respectively; the U direction was the observed governing direction (Figure 3c). The adaptive strategy tested the V direction first, and all 10,000 sampling paths selected W as the second direction. After V and W were tested, the mean posterior conformance probability at Stage 2 was 0.996, and all paths reached an acceptance decision at that stage; the U direction was not tested. UVW9 tested all three directions and rejected the group because the U-direction specimen-set mean fell below the threshold (Figure 3d). Printing group 18129 contributed 5.56 percentage points to the overall observed false-acceptance rate of the early-acceptance strategy, accounting for 60.7% of the overall rate of 9.15%.

Upon removal of the held-out evaluation records of Laboratory 18124, the false-acceptance rates of the early-acceptance strategy and UVW9 became 3.80% and 5.22%, respectively, with a difference of −1.42 percentage points. The joint assessment of Conditions (1) through (3) changed from unmet to met. Removal of the held-out evaluation records of any other laboratory did not change this assessment.

4.6. Decision Performance of the Restricted-Direction Strategy

In the present 34 printing groups, the restricted-direction strategy yielded group-by-group decisions identical to those of UVW9; both strategies had an observed false-acceptance rate of 4.93%. No false-rejection events were observed among the 16 reference-conforming printing groups for either strategy. The expected specimen count of the restricted-direction strategy was 6.49, with a laboratory-clustered 95% interval of 5.41 to 7.49, representing a 27.9% reduction (95% interval 16.8% to 39.9%) relative to the nine-specimen complete-direction testing (Table 3, Figure 3a). The point estimate of the expected

specimen count was below the 6.75 efficiency benchmark, while the upper bound of the interval exceeded this benchmark.

4.7. Incremental Effect of Testing Order and Efficiency Applicability Conditions

Under the restricted-direction strategy, the expected specimen counts were 6.96 under the prespecified W–V–U order, 6.49 under adaptive ordering, and 6.47 under the fixed V–W–U order. Relative to the W–V–U order, adaptive ordering saved 0.47 specimens per printing group (laboratory-clustered 95% interval 0.15 to 0.81; Figure 3b): 22 of the 34 printing groups had the same expected count under both orderings, 9 were lower under adaptive ordering, and 3 were lower under the fixed order. Relative to the fixed V–W–U order, by contrast, adaptive ordering offered no further saving: the paired difference was 0.01 specimens in favor of the fixed order (95% interval 0.00 to 0.03), decisions were identical, and only 3 of the 34 printing groups differed in expected count. The ordering-related saving therefore comes from testing the most frequently governing direction first, rather than from path-specific adaptation.

In the present evaluation set, the specimen savings observed under the restricted-direction strategy were concentrated in reference-nonconforming printing groups. The conditional expected specimen count for the 16 reference-conforming printing groups was 9.00, and for the reference-nonconforming printing groups it was 4.25 (Figure 4a). The point estimate of the reference-conforming-rate boundary corresponding to a 25% specimen reduction was 52.6%, with a laboratory-clustered 95% interval of 41.9% to 59.4%. The reference-conforming rate of the present evaluation set was 47.1%, below the boundary point estimate but within its 95% interval.

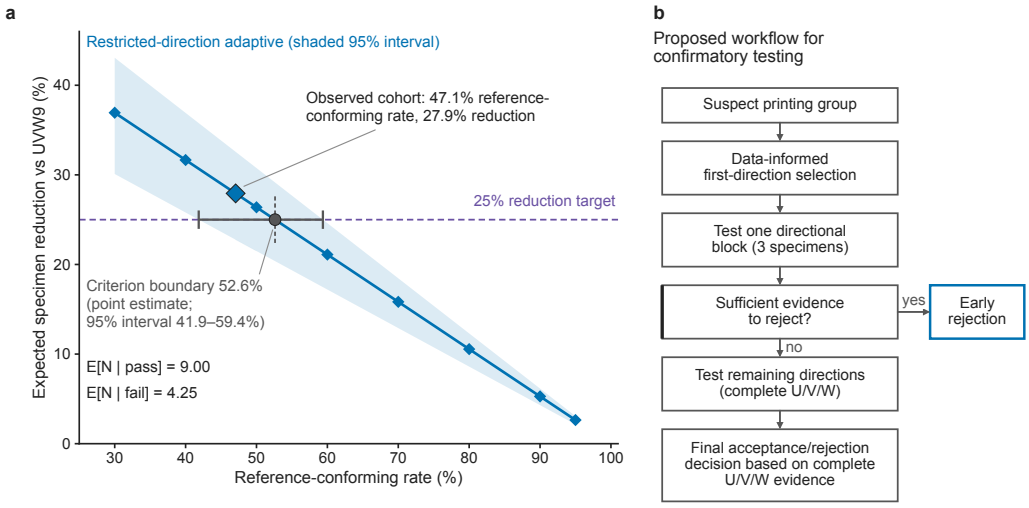


Figure 4. Efficiency of the restricted-direction strategy: (**a**) expected specimen reduction versus reference-conforming rate for the adaptive restricted-direction strategy, drawn as a blue line with small diamonds; the shaded blue band is the laboratory-clustered 95% interval, the large blue diamond marks the observed evaluation cohort (47.1% reference-conforming, 27.9% reduction), the purple horizontal dashed line marks the 25% reduction benchmark, and the grey circle with its horizontal whisker and vertical dashed line marks the reference-conforming rate at which that benchmark is reached (point estimate 52.6%, 95% interval 41.9% to 59.4%); and (**b**) the testing workflow in which partial-direction evidence may trigger early rejection (blue frame), whereas final acceptance requires complete U/V/W results.

5. Discussion

5.1. Directional Variability and Group-Level Acceptance Decisions

Previous studies have characterized the directional mechanical properties of 3DPC primarily through population-level mean comparisons. Some studies report that the direction normal to the deposited layers exhibits lower compressive strength, while others have observed different directional rankings [4,10,12]. Mix design, interlayer bonding, pore structure, printing parameters, and specimen size can all alter the magnitude and ranking of directional differences [7,9,13]. The present study further shows that population-level directional ranking and group-level acceptance decisions are distinct problems. Although the V direction was the observed governing direction in 20 of the 34 printing groups, the governing direction in the remaining 14 groups was U or W. The direction that is statistically weaker at the population level can therefore serve as a priority testing direction, but it cannot guarantee coverage of every printing group's lowest directional strength.

The exact enumeration of the fixed-direction strategies illustrates this distinction: at 40 MPa, V3 and VW6 showed higher false-acceptance rates than UVW9 (13.7% and 10.6% versus 4.9%), and single-direction testing overestimated mean strength by 3.00 to 8.14 MPa. Greater directional coverage requires more specimens, but it also improves the chance of detecting a printing group's lowest-strength direction. Directional rankings derived from historical data are suitable for determining the testing order, whereas group-level acceptance confirmation requires consideration of whether the directional evidence is complete.

5.2. Evidence Boundaries of the Early-Acceptance Strategy

The early-acceptance strategy reduced the expected specimen count by 44.8%, but its observed false-acceptance rate was 9.15%, exceeding 4.93% for UVW9 and failing to meet the risk criteria. The efficiency gain of early acceptance was thus obtained at the price of nearly doubling the observed false-acceptance rate; this risk–efficiency trade-off is central to the strategy. The 95% interval for the risk difference was $[-2.90, 18.30]$ percentage points, reflecting limited precision in estimating the population-level risk difference from the current sample. Under the available evidence, these results argue against adopting the early-acceptance rule examined in this study, but they do not establish that the direction of the risk difference would be the same across all laboratories, material systems, and printing conditions.

Printing group 18129 illustrates one type of information gap associated with partial-direction observation. The V and W direction means of this group substantially exceeded the threshold, causing the posterior conformance probability at Stage 2 to reach 0.996, while the untested U-direction mean was below the threshold. Cross-directional statistical associations can provide predictive information for untested directions but do not eliminate the uncertainty arising from within-group directional variability. This case illustrates one specific false-acceptance pathway; it does not imply that the entire 4.22-percentage-point strategy difference was attributable to Stage 2 stopping. The early-acceptance strategy used a posterior probability-based decision rule even after testing all three directions, whereas UVW9 used the minimum of the three directional specimen-set means; the 4.22 percentage points should therefore be interpreted as the difference between the two overall decision strategies.

The distribution of false-acceptance outcomes was uneven across laboratories. Printing group 18129 contributed 60.7% of the total observed false-acceptance rate of the early-acceptance strategy. Upon removal of the held-out evaluation records of Laboratory 18124, the risk difference changed from 4.22 to -1.42 percentage points. This influence analysis did not re-estimate the model parameters for the remaining cross-validation rounds and reflects the sensitivity of the evaluation results to the held-out records of Laboratory 18124. The current data are sufficient to show that the examined strategy did not meet the prespecified

criteria, but, given the wide risk-difference interval, additional independent data are needed to estimate the magnitude and direction of the population-level risk difference.

5.3. Decision Structure and Efficiency Conditions of the Restricted-Direction Strategy

The acceptance set of the restricted-direction strategy is a subset of the acceptance set of UVW9. The probabilistic model is used only to determine the direction testing order and to trigger early rejection; final acceptance still requires the complete U, V, and W decision rule. Consequently, even if the directional predictions or posterior probabilities contain bias, that bias cannot produce acceptance decisions beyond those of UVW9 through an early-acceptance pathway. This property is determined by the structure of the decision rule and does not depend on whether the current 34 printing groups happen to yield the same group-by-group decisions. The trade-off is that reference-conforming printing groups may be falsely rejected at an early stage. No such events were observed among the 16 reference-conforming printing groups in this study, but this sample is too small to conclude that the population-level false-rejection rate is zero.

Conventional concrete acceptance sampling controls producer's risk and consumer's risk by increasing the number of specimens within a batch [15,38], while Bayesian acceptance methods incorporate historical data to update the strength distribution and the decision probability [17,18]. These methods generally treat additional specimens as exchangeable observations from a single population. Directional testing of 3DPC differs in that each additional direction introduces a new candidate governing direction rather than a further replicate of one already tested [19,21]. The restricted-direction strategy uses historical information to improve testing efficiency while maintaining the complete-direction evidence requirement for final acceptance, offering a sequential approach suited to non-interchangeable directional observations.

The expected specimen count of the restricted-direction strategy was 6.49, a 27.9% reduction (95% interval 16.8% to 39.9%) relative to complete-direction testing, but the observed specimen savings were concentrated in reference-nonconforming printing groups. The conditional expected specimen count for reference-conforming printing groups was 9.00; consequently, overall efficiency depends on the proportion of conforming groups in the testing population. Because the reference-conforming rate of the present evaluation set (47.1%) lay below the boundary point estimate of 52.6% but within its 95% interval, the 25% reduction should be read as a point-estimate result specific to the current data. The interval for the reduction spans the 25% benchmark, so the reduction attainable in a different testing population could be materially smaller or larger than the point estimate. Testing order contributed a smaller share of the efficiency than the stopping rule: adaptive ordering saved 0.47 specimens per printing group relative to the W–V–U order (95% interval 0.15 to 0.81), and a fixed V–W–U order that places the most frequently governing direction first achieved the same performance (paired difference from adaptive ordering 0.01 specimens, 95% interval 0.00 to 0.03). A fixed order that begins with the most frequently governing direction therefore captures essentially all of the ordering-related efficiency, while the stopping rule determines when testing ends.

5.4. Implementation Context for Production Quality Control

The restricted-direction strategy is intended to operate within existing project-level acceptance requirements, for staged testing of printing groups whose conformance is in question. In a routine quality-control program, the procedure summarized in Figure 4b can serve as a screening tier within the existing acceptance workflow: printing groups enter the staged sequence as part of scheduled testing; early rejection diverts questionable groups to review or process investigation without waiting for complete directional results; and

groups that pass the early stages complete all three directions before acceptance. A possible implementation proceeds as follows. Before testing, the strength threshold is determined from the design or acceptance documents, and the first testing direction is selected based on historical U, V, and W strength data for the production line. If the results of the first or second direction trigger the early-rejection condition, acceptance of the printing group is withheld pending review, additional testing, or process investigation. Printing groups that do not trigger early rejection proceed to complete all three directions, with final acceptance based on the complete directional results. Complete-direction testing results can also be used periodically to update the direction ordering and model parameters. This procedure uses the statistical model to arrange the testing order and to identify potentially nonconforming conditions, without changing the directional evidence required for final acceptance. For routine implementation, a fixed order that begins with the direction most frequently governing on the production line is preferable to path-specific adaptive ordering. It requires no per-group posterior computation to select the next direction, is simpler to document within a quality-control procedure, and in the present data produced the same decisions and essentially the same specimen consumption (6.47 versus 6.49 specimens; Figure 3b). The order can be reviewed periodically as complete-direction results accumulate, rather than recomputed for each printing group.

Potential application scenarios for this procedure include trial production of new materials or mix designs, printing parameter adjustments, post-maintenance equipment verification, and quality investigation following anomalies detected by in-process monitoring [39–42]. Because these stages may have a higher nonconforming rate than stable production, early rejection is more likely to yield specimen savings in these settings. For production lines with stable processes and high conforming rates, most printing groups will still require three-direction testing, and the efficiency advantage of the restricted-direction strategy will diminish accordingly. The figure of 6.49 is an expected value averaged over printing groups and sampling paths; the actual count for any individual printing group remains 3, 6, or 9.

Sequential testing reduces the expected specimen consumption, not necessarily the decision turnaround time. If specimens for all three directions are typically prepared simultaneously and tested in parallel, waiting for the results of a preceding stage before initiating the next direction may extend the decision cycle for a printing group. If directional specimens can be prepared or tested in stages, the preparation and testing effort for unused specimens may be avoided. Production evaluation should therefore record, in addition to false-acceptance rate, false-rejection rate, and specimen count, the specimen extraction method, testing cycle, hold period, and process investigation cost, to assess whether the sequential procedure offers an overall efficiency advantage.

5.5. Study Limitations and Validation Needs

The available evidence was limited in both sample size and representativeness. The sample of 34 printing groups from 27 laboratories was insufficient to estimate the population-level risk difference precisely, as directly reflected by the paired interval width exceeding 20 percentage points. In addition, 20 of the 27 laboratories contributed a single printing group, so between-laboratory and between-group variation cannot be separated for most laboratories. The completeness requirement also excluded 10 of the 44 candidate printing groups, and the excluded groups differed from the retained ones, most prominently in the number of specimens per group, so the evaluation set cannot be regarded as a random sample of all printed groups. The interlaboratory data covered a range of materials, equipment, and specimen preparation conditions but lacked the batch timing, equipment status, environmental conditions, and in-process monitoring information typical

of continuous industrial production. Differences among laboratories in mix design, printing equipment, specimen size, and curing conditions were also not modeled separately. The current results therefore reflect a retrospective strategy evaluation under interlaboratory conditions, and the false-acceptance probabilities and testing schedule on an actual production line must be determined from field data. Validation on production-scale printing data is therefore a prerequisite for adopting the restricted-direction strategy in acceptance practice, rather than a refinement to be undertaken after adoption.

The sequential strategies also depend on the directional joint model and parameter estimation. The MCMC sensitivity analysis produced similar point estimates; the convergence warnings that appeared in some cross-validation rounds under the original sampling settings were resolved by reinforced sampling with no material change in the results (Table S2). The thresholds of 37.5 and 40.0 MPa were used to form approximately balanced evaluation operating points; specific projects should use externally determined acceptance thresholds. The conforming-rate boundary analysis held the empirical conditional expected specimen counts for reference-conforming and reference-nonconforming groups constant; changes in production conditions, stopping thresholds, or model configuration could shift the boundary position. Future studies should prespecify the printing-group definition, direction definitions, strength thresholds, and stopping rules before evaluation on independent production data. They should record complete-direction reference results, both types of misclassification, testing time, and specimen consumption throughout, and verify the decision performance and production applicability of the restricted-direction strategy in a prospective evaluation.

6. Conclusions

This study evaluated fixed-direction coverage strategies, a sequential strategy permitting early acceptance, and a restricted-direction strategy permitting early rejection only, using data from 27 laboratories, 34 printing groups, and 907 directional compressive test specimens. The main conclusions are as follows.

(1) The observed governing direction of a printing group was not fixed. V, W, and U were the observed governing directions in 20, 10, and 4 printing groups, respectively. At an operational threshold of 40 MPa, the observed false-acceptance rates of the single-direction V3 strategy and the two-direction VW6 strategy were 13.7% and 10.6%, respectively, both exceeding 4.9% for the complete-direction UVW9 baseline. Historical data can be used to identify priority testing directions, but reducing directional coverage increases the risk of missing the lowest directional strength of a printing group.

(2) The sequential strategy permitting early acceptance reduced the expected specimen count from 9.00 to 4.97, a reduction of 44.8%, but its observed false-acceptance rate was 9.15%, exceeding 4.93% for UVW9. The observed risk difference was 4.22 percentage points, with the point estimate exceeding the prespecified screening criterion of 2.5 percentage points; accordingly, this strategy did not meet the risk evaluation criteria. The paired 95% interval for the risk difference was $[-2.90, 18.30]$ percentage points, and the evaluation results were sensitive to the records of individual laboratories, indicating that the available data were insufficient to precisely estimate the population-level risk difference.

(3) The restricted-direction strategy limits the role of the probabilistic model to determining the direction testing order and triggering early rejection; final acceptance still requires complete testing in the U, V, and W directions. Under this decision structure, the acceptance set of the restricted-direction strategy cannot exceed that of UVW9; directional prediction bias therefore cannot introduce additional acceptance decisions.

In the present evaluation set, the restricted-direction strategy yielded group-by-group decisions identical to those of UVW9, with an expected specimen count of 6.49 (95% interval 5.41 to 7.49), a 27.9% reduction (95% interval 16.8% to 39.9%) relative to complete-direction testing. These results indicate that specimen consumption can be partially reduced through early identification of nonconforming printing groups while retaining complete directional evidence for acceptance.

(4) The efficiency of the restricted-direction strategy arises primarily from early rejection of reference-nonconforming printing groups; reference-conforming printing groups still require testing of all nine specimens. The overall efficiency therefore depends on the conforming-group proportion in the testing population. The point estimate of the reference-conforming-rate boundary for a 25% specimen reduction was 52.6%, with a 95% interval of 41.9% to 59.4%. Adaptive direction ordering reduced the expected specimen count by 0.47 specimens relative to the W–V–U order (95% interval 0.15 to 0.81), and a fixed order testing the most frequently governing direction first achieved the same reduction; path-specific adaptation provided no additional saving. These findings indicate that, in the directional strength acceptance scenario examined here, cross-directional historical information should be used to arrange the testing order and to identify nonconforming printing groups early, whereas final acceptance should continue to require complete directional evidence.

In practice, the restricted-direction strategy can be applied within existing project-level acceptance requirements, using a fixed testing order that begins with the direction most frequently governing on the production line and reserving the probabilistic model for ordering and early rejection. Field validation on production-scale printing data remains a prerequisite before the approach is adopted for acceptance decisions.

Supplementary Materials: The following supporting information can be downloaded at: https://www.mdpi.com/article/10.3390/civileng7030062/s1, Figure S1: Quantile–quantile plots of the natural logarithm of the arithmetic mean of the raw strength measurements within each printing group and direction, against the standard normal distribution (34 printing groups per direction): (a) direction U; (b) direction V; (c) direction W. The annotations report the p-values of the Shapiro–Wilk and D'Agostino K^2 tests for each direction. Tests of the joint three-direction distribution lead to the same conclusion (Mardia skewness $p = 0.59$, Mardia kurtosis $p = 0.70$, Henze–Zirkler $p = 0.37$). With 34 groups per direction, the power of these diagnostics to detect moderate departures is limited. Table S1: Sensitivity of the early-acceptance strategy. Each row varies one factor relative to the primary configuration, which uses acceptance and rejection confidence thresholds of 0.90/0.90, loss weights $c_{FA}/c_{FR} = 0.65/0.35$ with the acceptance probability cutoff $p^* = 0.65$, and 10,000 sampling paths per printing group. The false-acceptance rate is the mean acceptance probability over the 18 reference-nonconforming printing groups at the per-round primary operating thresholds; the increment is expressed in percentage points (pp) relative to the complete-direction UVW9 baseline evaluated on the same groups; the expected specimen count is averaged over all 34 printing groups; and the reduction is relative to the nine-specimen UVW9 baseline. Table S2: Convergence diagnostics of the hierarchical Bayesian model by leave-one-laboratory-out round, under the original sampling settings (four chains, 1000 draws and 1500 warmup iterations per chain) and after reinforced sampling (four chains, 4000 draws and 4000 warmup iterations per chain). Rows list the rounds in which at least one diagnostic fell outside its limit under the original settings (maximum R-hat above 1.01, minimum bulk ESS below 400, or minimum tail ESS below 400), ordered by the identifier of the held-out laboratory; the final row summarizes the remaining rounds. For each round, the maximum R-hat and the minimum bulk and tail effective sample sizes (ESS) are taken over all model parameters.

Author Contributions: Conceptualization, L.J., S.S. and B.N.; methodology, L.J. and S.S.; software, L.J. and S.S.; validation, L.J., S.S. and Z.H.; formal analysis, L.J. and S.S.; investigation, L.J., S.S. and Z.Z.; resources, Z.Z. and B.N.; data curation, L.J. and S.S.; writing—original draft preparation, L.J. and S.S.; writing—review and editing, Z.H., Z.Z. and B.N.; visualization, L.J. and S.S.; supervision, B.N.; project administration, B.N.; funding acquisition, B.N. Authors L.J. and S.S. contributed equally to this work and share first authorship. All authors have read and agreed to the published version of the manuscript.

Funding: This research was funded by the National Key Research Project, grant number H2026249, and the Key Research and Development Program of Liaoning Province, grant number LJ212610157037.

Data Availability Statement: The core analysis code, parameter configurations, and evaluation scripts supporting this study are available at https://github.com/BrewSSS/3dpc-sequential-acceptance (accessed on 23 August 2026). The underlying interlaboratory data are available through the RILEM TC 304-ADC database [22].

Acknowledgments: During the preparation of this manuscript, the authors used DeepSeek V4 Flash for language editing. The authors reviewed and edited the output as needed and take full responsibility for the content of this publication.

Conflicts of Interest: The authors declare no conflicts of interest.

Abbreviations

The following abbreviations are used in this manuscript:

3DPC	3D-printed concrete
LOLO	leave-one-laboratory-out
MAD	median absolute deviation
MCMC	Markov chain Monte Carlo
PCHIP	piecewise cubic Hermite interpolation

References

1. Nerella, V.N.; Hempel, S.; Mechtcherine, V. Effects of layer-interface properties on mechanical performance of concrete elements produced by extrusion-based 3D-printing. *Constr. Build. Mater.* **2019**, *205*, 586–601. [CrossRef]
2. Kolawole, J.T.; Buswell, R.; Mahmood, S.; Isa, M.N.; Cavalaro, S.; Austin, S.; Engelberg, D.; Dobrzanski, J.; Xu, J.; Withers, P.J. On the origins of anisotropy of extrusion-based 3D printed concrete: The roles of filament skin and agglomeration. *Cem. Concr. Res.* **2025**, *192*, 107817. [CrossRef]
3. Bos, F.; Menna, C.; Robens-Radermacher, A.; Wolfs, R.; Roussel, N.; Lombois-Burger, H.; Baz, B.; Weger, D.; Nematollahi, B.; Santhanam, M.; et al. Mechanical properties of 3D printed concrete: A RILEM TC 304-ADC interlaboratory study—Approach and main results. *Mater. Struct.* **2025**, *58*, 183. [CrossRef]
4. Mechtcherine, V.; Muthukrishnan, S.; Robens-Radermacher, A.; Wolfs, R.; Versteege, J.; Menna, C.; Ozturk, O.; Ozyurt, N.; Roupec, J.; Richter, C.; et al. Mechanical properties of 3D printed concrete: A RILEM 304-ADC interlaboratory study—Compressive strength and modulus of elasticity. *Mater. Struct.* **2025**, *58*, 181. [CrossRef]
5. *EN 12390-3:2019*; Testing Hardened Concrete—Part 3: Compressive Strength of Test Specimens. European Committee for Standardization (CEN): Brussels, Belgium, 2019.
6. *ASTM C39/C39M-24*; Standard Test Method for Compressive Strength of Cylindrical Concrete Specimens. ASTM International: West Conshohocken, PA, USA, 2024. [CrossRef]
7. Aminpour, N.; Memari, A. Analysis of anisotropic behavior in 3D concrete printing for mechanical property evaluation. *J. Build. Eng.* **2025**, *99*, 111652. [CrossRef]
8. Yu, Q.; Zhu, B.; Liu, X.; Chen, W.; Zhang, Y.; Pan, J. Pore morphology and orientation-induced mechanical orthotropic behavior of 3D-printed concrete filament. *J. Mater. Civ. Eng.* **2026**, *38*, 04026095. [CrossRef]
9. Moelich, G.M.; Kruger, J.; Combrinck, R. Modelling the interlayer bond strength of 3D printed concrete with surface moisture. *Cem. Concr. Res.* **2021**, *150*, 106559. [CrossRef]
10. Cheng, H.; Aljuwayhel, F.N.; Chu, S.H.; Radlińska, A. Directional pore structure governs compressive anisotropy in 3D printed concrete. *Cem. Concr. Compos.* **2026**, *171*, 106640. [CrossRef]

11. Ma, G.; Li, Z.; Wang, L.; Wang, F.; Sanjayan, J. Mechanical anisotropy of aligned fiber reinforced composite for extrusion-based 3D printing. *Constr. Build. Mater.* **2019**, *202*, 770–783. [CrossRef]
12. Bai, M.; Xiao, J.; Shen, J.; Ding, T.; Chen, W. Printability and mechanical anisotropy of 3D-printed concrete with manufactured sand derived from basalt. *3D Print. Addit. Manuf.* **2025**, *12*, 413–424. [CrossRef] [PubMed]
13. Tay, Y.W.D.; Ting, G.H.A.; Qian, Y.; Panda, B.; He, L.; Tan, M.J. Time gap effect on bond strength of 3D-printed concrete. *Virtual Phys. Prototyp.* **2019**, *14*, 104–113. [CrossRef]
14. Li, K.S. A compound sampling scheme for acceptance testing of concrete. *Mater. Struct.* **1993**, *26*, 517–521. [CrossRef]
15. Caspeele, R.; Taerwe, L. Probabilistic evaluation of conformity criteria for concrete families. *Mater. Struct.* **2011**, *44*, 1219–1231. [CrossRef]
16. *EN 206:2013+A2:2021*; Concrete—Specification, Performance, Production and Conformity. European Committee for Standardization (CEN): Brussels, Belgium, 2021.
17. Caspeele, R.; Taerwe, L. Bayesian assessment of the characteristic concrete compressive strength using combined vague–informative priors. *Constr. Build. Mater.* **2012**, *28*, 342–350. [CrossRef]
18. Caspeele, R.; Taerwe, L. Numerical Bayesian updating of prior distributions for concrete strength properties considering conformity control. *Adv. Concr. Constr.* **2013**, *1*, 85–102. [CrossRef]
19. Wald, A. Sequential tests of statistical hypotheses. *Ann. Math. Stat.* **1945**, *16*, 117–186. [CrossRef]
20. Wald, A.; Wolfowitz, J. Optimum character of the sequential probability ratio test. *Ann. Math. Stat.* **1948**, *19*, 326–339. [CrossRef]
21. *ISO 28591:2017*; Sequential Sampling Plans for Inspection by Attributes. International Organization for Standardization: Geneva, Switzerland, 2017.
22. Robens-Radermacher, A.; Kujath, C.; Bos, F.; Mechtcherine, V.; Unger, J.F. Mechanical properties of 3D printed concrete: A RILEM TC 304-ADC interlaboratory study—Design and implementation of a database system for querying, sharing, and analyzing experimental data. *Mater. Struct.* **2025**, *58*, 184. [CrossRef]
23. Gelman, A.; Carlin, J.B.; Stern, H.S.; Dunson, D.B.; Vehtari, A.; Rubin, D.B. *Bayesian Data Analysis*, 3rd ed.; Texts in Statistical Science; CRC Press: Boca Raton, FL, USA, 2013.
24. Rousseeuw, P.J.; Croux, C. Alternatives to the median absolute deviation. *J. Am. Stat. Assoc.* **1993**, *88*, 1273–1283. [CrossRef]
25. Virtanen, P.; Gommers, R.; Oliphant, T.E.; Haberland, M.; Reddy, T.; Cournapeau, D.; Burovski, E.; Peterson, P.; Weckesser, W.; Bright, J.; et al. SciPy 1.0: Fundamental algorithms for scientific computing in Python. *Nat. Methods* **2020**, *17*, 261–272. [CrossRef] [PubMed]
26. Genz, A. Numerical computation of multivariate normal probabilities. *J. Comput. Graph. Stat.* **1992**, *1*, 141–149. [CrossRef]
27. Berger, J.O. *Statistical Decision Theory and Bayesian Analysis*, 2nd ed.; Springer Series in Statistics; Springer: New York, NY, USA, 1985. [CrossRef]
28. Fritsch, F.N.; Carlson, R.E. Monotone piecewise cubic interpolation. *SIAM J. Numer. Anal.* **1980**, *17*, 238–246. [CrossRef]
29. Roberts, D.R.; Bahn, V.; Ciuti, S.; Boyce, M.S.; Elith, J.; Guillera-Arroita, G.; Hauenstein, S.; Lahoz-Monfort, J.J.; Schröder, B.; Thuiller, W.; et al. Cross-validation strategies for data with temporal, spatial, hierarchical, or phylogenetic structure. *Ecography* **2017**, *40*, 913–929. [CrossRef]
30. Steyerberg, E.W.; Harrell, F.E. Prediction models need appropriate internal, internal–external, and external validation. *J. Clin. Epidemiol.* **2016**, *69*, 245–247. [CrossRef] [PubMed]
31. Efron, B. Bootstrap methods: Another look at the jackknife. *Ann. Stat.* **1979**, *7*, 1–26. [CrossRef]
32. Field, C.A.; Welsh, A.H. Bootstrapping clustered data. *J. R. Stat. Soc. Ser. B Stat. Methodol.* **2007**, *69*, 369–390. [CrossRef]
33. Abril-Pla, O.; Andreani, V.; Carroll, C.; Dong, L.; Fonnesbeck, C.J.; Kochurov, M.; Kumar, R.; Lao, J.; Luhmann, C.C.; Martin, O.A.; et al. PyMC: A modern, and comprehensive probabilistic programming framework in Python. *PeerJ Comput. Sci.* **2023**, *9*, e1516. [CrossRef] [PubMed]
34. Hoffman, M.D.; Gelman, A. The No-U-Turn sampler: Adaptively setting path lengths in Hamiltonian Monte Carlo. *J. Mach. Learn. Res.* **2014**, *15*, 1593–1623.
35. Lewandowski, D.; Kurowicka, D.; Joe, H. Generating random correlation matrices based on vines and extended onion method. *J. Multivar. Anal.* **2009**, *100*, 1989–2001. [CrossRef]
36. Vehtari, A.; Gelman, A.; Simpson, D.; Carpenter, B.; Bürkner, P.C. Rank-normalization, folding, and localization: An improved $\widehat{R}$ for assessing convergence of MCMC (with discussion). *Bayesian Anal.* **2021**, *16*, 667–718. [CrossRef]
37. Kumar, R.; Carroll, C.; Hartikainen, A.; Martin, O. ArviZ a unified library for exploratory analysis of Bayesian models in Python. *J. Open Source Softw.* **2019**, *4*, 1143. [CrossRef]
38. *ACI 214R-11*; Guide to Evaluation of Strength Test Results of Concrete. American Concrete Institute: Farmington Hills, MI, USA, 2011.
39. Mechtcherine, V.; van Tittelboom, K.; Kazemian, A.; Kreiger, E.; Nematollahi, B.; Nerella, V.N.; Santhanam, M.; de Schutter, G.; Van Zijl, G.; Lowke, D.; et al. A roadmap for quality control of hardening and hardened printed concrete. *Cem. Concr. Res.* **2022**, *157*, 106800. [CrossRef]

40. Bos, D.; Wolfs, R. A quality control framework for digital fabrication with concrete. *RILEM Tech. Lett.* **2023**, *8*, 106–112. [CrossRef]
41. Rill-García, R.; Dokladalova, E.; Dokládal, P.; Caron, J.F.; Mesnil, R.; Margerit, P.; Charrier, M. Inline monitoring of 3D concrete printing using computer vision. *Addit. Manuf.* **2022**, *60*, 103175. [CrossRef]
42. Kazemian, A.; Khoshnevis, B. Real-time extrusion quality monitoring techniques for construction 3D printing. *Constr. Build. Mater.* **2021**, *303*, 124520. [CrossRef]

Disclaimer/Publisher's Note: The statements, opinions and data contained in all publications are solely those of the individual author(s) and contributor(s) and not of MDPI and/or the editor(s). MDPI and/or the editor(s) disclaim responsibility for any injury to people or property resulting from any ideas, methods, instructions or products referred to in the content.